A SINGLE CAVITY ECHO SCHEME*

P. Gandhi†, X-W Gu‡, and J. Wurtele
University of California, Berkeley and Lawrence Berkeley National Laboratory, Berkeley, CA, USA
G. Penn and M. Reinsch
Lawrence Berkeley National Laboratory, Berkeley, CA, USA

Abstract

The possibility of implementing echo-enabled harmonic generation (EEHG) within a single optical resonance cavity is explored both analytically and with numerical simulations. Two modulators of the same frequency are used so that the cavity radiation replaces the two seed lasers of conventional EEHG. Such a scheme has potential to produce tunable radiation as in EEHG, but with the high repetition rate, longitudinal coherence, and narrow spectral bandwidth of an oscillator. These benefits, however, come with the complication that the beam must generate the radiation that modulates it. Analysis and GINGER simulations are presented for a specific example that takes advantage of robust multilayer mirror performance at 13.4 nm to produce radiation near or possibly even below 1 nm.

INTRODUCTION

Echo enabled harmonic generation (EEHG) has shown the potential to produce longitudinally coherent radiation at very high harmonics of given seed radiation [2]. Simulations based on this technique have produced radiation with a harmonic upshift of 50 [3] and higher [6], and it has even been demonstrated experimentally [5]. Wurtele et al. [7] have proposed several variations of this technique that make use of oscillators in an attempt to rid the scheme of the need for external seed lasers that could limit the repetition rate. This paper provides a simple and approximate analytic framework for choosing design parameters. The single cavity echo scheme uses a single resonance cavity to build up a single radiation pulse that is used for both modulating sections of the echo scheme as shown in Fig. 1. Because of the strength of the dispersion required by the echo scheme, the electron pulse would slip completely behind the radiation pulse if a simple two mirror cavity was used. The modified geometry shown in Fig. 1b would add extra path length for the light so that the electron bunch has a chance to catch up to the radiation pulse for the second modulation. A detailed study of the beam and photon optics would be required to put such a design in practice, but it may be useful when the available mirrors are lossy since it adds only one additional reflection. This study considers the two mirror geometry (Fig. 1a), and is time-independent so that the slippage effect can be ignored.

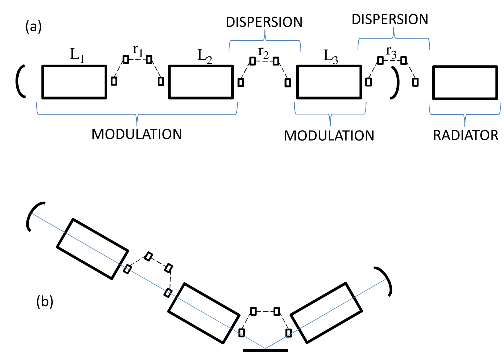

Figure 1: (a)A schematic of the proposed scheme with undulator lengths and chicane R_{56} strengths labeled. The purpose each section serves in terms of EEHG is also marked. (b) A modified geometry with a third mirror to increase the pathlength of the light to account for the slippage due to the strong chicane. Note that the angle is greatly exaggerated.

A SIMPLE TIME-INDEPENDENT, ONE-DIMENSIONAL THEORY

As with the optical klystron, this scheme relies on the spatial separation of the modulation, bunching, and radiation generation. This, along with the fact that each undulator section is short compared to the one-dimensional gain length, allows for many simplifications to the theory. Using a method similar to those applied to optical klystrons (see, for example, [1]), one can develop a theory to predict the values of the collective FEL variables (Eqns. 1) at the end of each section of the scheme. The results of such a theory are summarized in Table 1.

$$a = \frac{\omega}{\omega_p\sqrt{\rho\gamma_0}}\frac{eE}{km_ec^2},\ b = \langle e^{-i\theta}\rangle,\ p = \langle \eta e^{-i\theta}\rangle \qquad (1)$$

The following conventions are used: $\theta = (k+k_w)z-ckt$ is the pondermotive phase, $\eta = \gamma-\gamma_0/\rho\gamma_0$ is the scaled fractional energy, and the distance along the undulator is scaled by $z \to 2k_w\rho z$. $k_w = 2\pi/\lambda_w$ is the wiggler wavenumber, $k = 2\pi/\lambda$ is the radiation wavenumber, $\omega_p^2 = 4\pi e^2 n_e/m_e$, $\gamma_0^2 = \lambda_w(1+a_w^2)/2\lambda$ is the resonant electron beam energy,

* This work was supported by the DIrector, Office of Science, of the U.S. Department of Energy under Contract No. DE-AC02-05CH11231.
† punit_gandhi@berkeley.edu
‡ Currently at University of Electronic Science and Technology of China (UESTC) Institute of High Energy Electronics, Chengdu, Sichuan; China

Table 1: Summary of Collective Variables after Passing Through the Various Sections of the Scheme

	a	b	p
Initial	a_0	0	0
Undulator 1	a_0	0	$a_0 L_1$
Chicane 1	a_0	b_d	p_d
Undulator 2	$-b_d L_2 + a_0$	b_d	$-\frac{1}{2} b_d L_2^2 + a_0 L_2 + p_d$
Chicane 2	$-b_d L_2 + a_0$	0	0
Undulator 3	$-b_d L_2 + a_0$	0	$(-b_d L_2 + a_0) L_3$

and $a_w = eB_w/\sqrt{2} k_w m_e c^2$ is the rms undulator parameter, and the one-dimensional FEL parameter is given by

$$\rho_{1D} = \frac{1}{\gamma_0}\left[\frac{a_w \omega_p}{ck_w}\right]^{2/3} = \left[\frac{1}{16\pi}\frac{I}{I_A}\left(\frac{a_w [JJ]}{1+a_w^2}\right)^2 \frac{\gamma_0 \lambda}{\Sigma_A}\right]^{1/3} \quad (2)$$

where Σ_A is the rms cross sectional area of the electron beam.

An explicit expression for the bunching at the end of the chicane section is a standard result that can be found in, for example, [1] and the collective modulation can be calculated using a similar approach.

$$|b_d| = e^{-r_1^2 \sigma^2/2} J_1(2|a_0| r_1 L_1) \quad (3)$$

$$|p_d| = |b_d| \left(r_1 \sigma^2 - \frac{J_1'(2|a_0| r_1 L_1)}{J_1(2|a_0| r_1 L_1)} \right) \quad (4)$$

σ is defined to be the initial energy spread of the beam in units of the scaled energy η.

CONSTRAINTS

We will define A_1 to be the desired modulation amplitude (in units of initial energy spread σ) of the first modulation section. The saturated mode will be optimized for EEHG when $A_1 \approx 3$ [4]. We note that this may not always be possible as the energy modulation after undulator 2 must be larger than $a_0 L_1$, the modulation after undulator 1.

$$A_1 \sigma = \left| -\frac{1}{2} b_d L_2^2 + a_0 L_2 + p_d \right| \quad (5)$$

We need to consider our particular parameters to determine the optimum modulation for the second modulation section [4]. Given a target final radiation wavelength, a larger second modulation would reduce the strength of the required first chicane, but would induce a larger energy spread. The desired second modulation amplitude A_2 (in units of σ) must balance the difficulties of a strong chicane with the energy spread tolerance of the radiator.

$$A_2 \sigma = |-b_d L_2 L_3 + a_0 L_3| \quad (6)$$

A third constraint can be found by realizing that a steady state will only be reached within the the optical cavity if the total gain in the cavity exactly balances the losses. With the cavity losses defined by $aR = a_0$, a third constraint can be written as

$$|a_0| \left(\frac{1}{R} - 1\right) = |b_d| L_2 \quad (7)$$

where optimized phasing has been assumed.

PARAMETER OPTIMIZATION

For a transverse optical klystron, we have certain constraints and optimimum parameters. Using these relations along with the constraints from above, we can try to design an single cavity echo scheme. Start with the constraint on the dispersion strength of the optical klystron which is limited by the initial energy spread, $r_1 \lesssim 1/\sigma$. A stronger dispersion strength will allow for a shorter first undulator section and thus smaller modulation amplitude [1]. However, the slippage of the electrons relative to the light caused by the chicane may put a lower limit on the dispersion strength than the initial energy spread. While this analysis doesn't include time dependent effects, the slippage distance should be small compared to the length of the bunch if the scheme is to be successful in practice. Further limits from spectral broadening may be put on the chicane strength as well.

Once the dispersion strength is fixed, the optimum length of the first undulator section can be determined by maximizing the bunching coming out of the dispersion section. The Bessel Function $J_1(x)$ has a maximum value approximately 0.58 at $x_m \approx 1.84$, so that the undulator length should be

$$L_1 = \frac{x_m}{2|a_0| r_1} \quad (8)$$

Plugging these optimum values into the above constraints and solving for the field provides the following expression

$$|a_0| = \left[\frac{2|b_d| R^2}{1-R^2} (A_1 \sigma - |p_d|)\right]^{1/2} \quad (9)$$

where the collective bunching and modulation variables at the end of the first chicane can now be explicitly calculated from Eq. 3 and 4, respectively.

The lengths of the other two undulator sections then become

$$L_2 = \frac{1-R}{R}\frac{|a_0|}{|b_d|}, \; L_3 = \frac{A_2 \sigma R}{|a_0|} \quad (10)$$

A 13.4 NM EXAMPLE

In this section we consider a 13.4 nm example roughly based on beam parameters proposed for a new light source at LBNL [9]. We have chosen 2.4-GeV electron beam with a peak current of 150 A, an incoherent energy spread of 24 keV, and a transverse normalized emittance of 0.1 μm. Note the beam quality considered here is higher than proposed for LBNL FEL studies. Further work will be required to understand the limitations of the scheme

Table 2: Some Key Parameters for the Steady-state GINGER Simulations of a 13.4 nm Single Cavity Echo Scheme

First EEHG Modulation: (Optical Klystron)	Wiggler sections	2 identical
	λ_w	7 cm
	a_w	2.7
	Section 1 length	56 cm
	Section 2 length	133 cm
	Chicane length	118 cm
	R_{56}	213 μm
First EEHG Dispersion:	Length	118 cm
	R_{56}	2.2 mm
Second EEHG Modulation:	Wiggler sections	1 as above
	Section length	42 cm
Optical Cavity:	Cavity power	7.3 MW
	Losses/reflection	30%
Second EEHG Dispersion:	Length	118 cm
	R_{56}	121 μm
7.4 Å Radiator:	λ_w	1.1 cm
	a_w	1.4
	Length	11 m
	Power	270 MW

as the initial energy spread and emittance are increased. The undulator sections within the cavity all have a period of 7 cm and an rms undulator parameter of 2.7, making $\rho_{1D} = 3.4 \times 10^{-3}$. We reduce the gain by a ratio of the electron beam size to the radiation size of the cavity mode to account for the transverse mismatch of the two. We also assume a total field loss of 30% corresponding to state of the art multilayer mirror production at 13.4 nm [10].

Choosing the first modulation to be 3σ and the second modulation σ, the lengths of the sections predicted by the theory are (after converting back to dimensional units) $L_1 \approx 56$ cm, $L_2 \approx 133$ cm, and $L_3 \approx 42$ cm. The predicted saturated cavity field at the entrance of the undulator is $a \approx 0.15$ which corresponds to a power of 3.4 MW assuming a 150 μm waist for the laser.

GINGER [11] was used to conduct a time-independent simulation of the cavity for 200 passes, well after a steady state within the oscillator was reached. The output particles from the last pass of the simulation were then passed through a chicane and radiator in a separate GINGER simulation. The inputs and results of the simulation are summarized in Table 2.

The power within the oscillator cavity saturated at twice the value predicted by Eq. 9, and the energy spread of the beam at the exit of the cavity was about 4 times the target value. Even still, the phase space at the entrance of the radiator, shown in Fig. 2, looks promising as an implementation of EEHG. Approximately 270 MW of power at 0.74 nm was produced after about 11 m in the radiator. For comparison, A conventional echo scheme with modulation sizes of 3 and 1 times the initial energy spread produced roughly 285 MW and saturated at roughly the same distance.

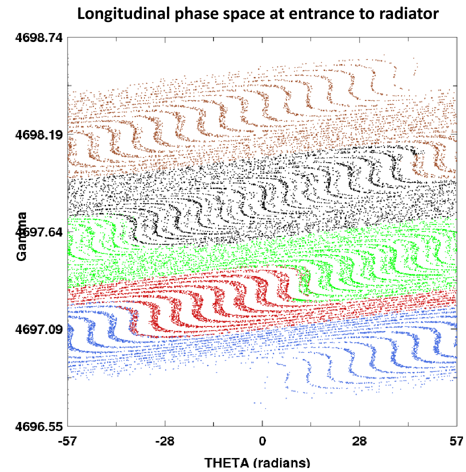

Figure 2: The electron phase space entering the radiator after going through the single oscillator echo scheme.

Interestingly, varying the strength of the strong dispersion r_2 had a dramatic impact on the dynamics of the oscillator cavity. While scanning the value of the R_{56} from 2 mm to 3 mm, it was noticed that the oscillator would not maintain power within the cavity at values of 2.4 mm or 2.6 mm, but had the same saturated cavity power of over 7 MW at 2 mm, 2.2 mm, 2.8 mm, and 3 mm.

CONCLUSIONS

A simple model for understanding the single cavity echo scheme can provide some insight into its steady state mode. Time-independent GINGER simulations show that this model provides design parameters that perform similar to EEHG using standard modulators for the case of a 13.4 nm oscillator used to generate sub-nanometer radiation. The theory developed here could be improved by including the effects of beam quality, time-dependence, and transverse dynamics.

REFERENCES

[1] R. Bonifacio et al. Phys Rev. A 45,6 (1992)

[2] G. Stupakov, Phys. Rev. Lett. **102**, 074801 (2009) .

[3] D. Xiang and G. Stupakov, SLAC-PUB-13645 (2009) .

[4] D. Xiang and G. Stupakov, SLAC-PUB-13644 (2009) .

[5] D. Xiang et al. *Phys. Rev. Lett.* 2010, 105, 114801-14.

[6] G. Penn and M Reinsch, Journal of Modern Optics (2011).

[7] J. Wurtele et al. Proc. of the 2010 FEL Conference.

[8] Z. Huang and K-J Kim, Phys Rev. ST Accel. Beams 10,034801 (2007) .

[9] J.N. Corlett *et al.*, Proc. FEL 2010 (Malmo, Sweden).

[10] D. Attwood, private communication.

[11] W.M. Fawley, LBNL CBP Tech Note-104 (1995).